

Spectral Properties of Stochastic Resonance in Quantum Transport

Robert Hussein¹, Sigmund Kohler², Johannes C. Bayer³, Timo Wagner³, and Rolf J. Haug³¹Fachbereich Physik, Universität Konstanz, D-78457 Konstanz, Germany²Instituto de Ciencia de Materiales de Madrid, CSIC, E-28049 Madrid, Spain³Institut für Festkörperphysik, Leibniz Universität Hannover, D-30167 Hanover, Germany (Received 24 June 2020; accepted 15 October 2020; published 10 November 2020)

We investigate theoretically and experimentally stochastic resonance in a quantum dot coupled to electron source and drain via time-dependent tunnel barriers. A central finding is a transition visible in the current noise spectrum as a bifurcation of a dip originally at zero frequency. The transition occurs close to the stochastic resonance working point and relates to quantized pumping. For the evaluation of power spectra from measured waiting times, we generalize a result from renewal theory to the ac-driven case. Moreover, we develop a master equation method to obtain phase-averaged current noise spectra for driven quantum transport.

DOI: 10.1103/PhysRevLett.125.206801

Stochastic resonance (SR) is a counterintuitive phenomenon by which the output signal of a device improves due to the action of external noise [1,2]. Typically, it emerges as an interplay of periodic driving, nonlinearities, and noise-induced activation. The paradigmatic example consists of two states separated by an energetic barrier, where an external oscillating force causes periodic transitions considered as signal. When the force is rather weak, noise may help to cross the barrier and, thus, improves the signal. For very strong noise, however, the output inherits too much randomness and degrades. This reflects a prominent feature of SR, namely an optimal working point at an intermediate noise level. Typically SR occurs when the driving frequency roughly matches one half of the intrinsic decay rate of the system $f = \Gamma_0/2$ [2]. SR has been suggested as the mechanism behind very different phenomena ranging from the periodic recurrence of ice ages to biological signal processing [3]. Many of these ideas have been realized experimentally in the classical regime, while the quantum regime has been explored mainly theoretically [4–6].

Recently in an experiment with a biased quantum dot with time-dependent tunnel rates, SR has been extended to the realm of quantum transport with the zero-frequency noise of the current as a measure for the signal quality [7]. It turned out that the current noise indeed assumes its minimum when the driving frequency obeys the mentioned SR condition. However, as only zero-frequency properties of the experimental data were evaluated, the question arises whether additional information can be extracted from the full power spectrum of the current fluctuations.

With this Letter, we demonstrate that the current noise spectrum provides relevant insight to SR in quantum transport. We develop a method for computing the frequency-dependent Fano factor [8–10] for ac-driven transport and compare the results with experimental data from

an ac-driven quantum dot similar to Ref. [7]. For the data analysis, we generalize the relation between waiting times and the power spectrum of a spike train known from renewal theory [11,12] to the ac-driven case. Finally, we discuss possible applications for quantized charge pumping and current standards [13–16].

Experimental setup and model.—We employ a Schottky gate defined quantum dot based on the two-dimensional electron gas of a GaAs/AlGaAs heterostructure at 1.5 K shown in Fig. 1(a). The current I_{QPC} through an adjacent

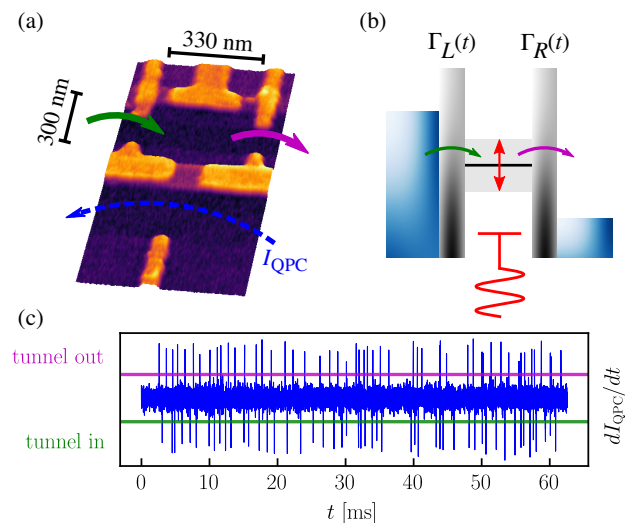


FIG. 1. (a) Strongly biased quantum dot with periodically time-dependent tunnel couplings. It can be charged by electrons entering from the source (green arrow) and discharged toward the drain (magenta). The quantum point contact measures the dot occupation. (b) Corresponding theoretical model. (c) Time derivative of I_{QPC} . The sign of the spikes reflects the change of the dot occupation.

quantum point contact monitors the charge on the quantum dot. Low capacitance (25 pF) coaxial lines and a high bandwidth (100 kHz) transimpedance amplifier are used to ensure an electronic bandwidth well above the experimental timescales. By applying sufficiently negative voltages to the center gates, the visible gap in the center is electrostatically closed and the two paths are galvanically isolated. From the upper side, the quantum dot is confined by two tunnel barrier gates and a plunger gate, which are used to manipulate the tunneling rates and the energy levels.

The quantum dot is tunnel coupled to biased leads, where gate voltages are applied such that its lowest level, hosting up to one electron, lies in the center of the bias window. Care has been taken to tune the dot to a symmetric coupling to source and drain, such that without the driving, the tunnel rates from the source and to the drain are equal. The ac components of the gate voltages let the dot level oscillate as sketched in Fig. 1(b), and the tunnel rates become time dependent [7,16]. We model this system by golden-rule rates with an exponential dependence on the oscillating gate voltages,

$$\Gamma_{L/R}(t) = \Gamma_0 \exp[\pm \alpha_{L/R} A \cos(\Omega t)], \quad (1)$$

where driving amplitude and period are A and $T = 2\pi/\Omega \equiv 1/f$, respectively. The leverage factors $\alpha_{L/R}$ and the intrinsic decay rate Γ_0 are adjusted such that the $\Gamma_{L/R}(t)$ match the rates in the experiment. Since in our sample $\alpha_L \neq \alpha_R$, the system possess a slight asymmetry which grows with the amplitude. Transport phenomena in this open system can be described by a master equation of the form $\dot{\rho} = \mathcal{L}(t)\rho$, where ρ is the reduced density operator of the central conductor with the T -periodic Liouvillian $\mathcal{L}(t) = \mathcal{L}(t+T)$.

Current measurements are affected by displacement currents of the fluctuating charge configuration [17,18], in our case, of the stochastic charging and discharging of the quantum dot. Therefore, one has to distinguish the particle currents at the interfaces, I_L and I_R , from the total (or Ramo-Shockley) current $I_{\text{tot}} = -\kappa_L I_L + \kappa_R I_R$ in the leads [19,20]. κ_L and $\kappa_R = 1 - \kappa_L$ are normalized gate capacitances which we assume time independent and symmetric, $\kappa_L = \kappa_R = 1/2$. While this distinction is irrelevant for the average current \bar{I} and the zero-frequency noise [21], it is quite important for the current noise spectrum [9,19].

In the experiment, the charge monitor records the dot occupation which changes by electron tunneling. For large bias, tunneling to the dot can be assigned to the particle current at the source I_L , while discharging the dot corresponds to I_R . Therefore, the time derivative of the current through the point contact shown in Fig. 1(c) is a train of negative (positive) spikes which represent a realization of the stochastic process underlying the particle current at the

source (drain), while both spike trains together correspond to the total current. Thus, in contrast to traditional measurements in the leads, the charge monitor provides also the particle currents $I_{L/R}$. Here, we focus on the total current, because it turns out that its noise spectrum S_{tot} is most significantly affected by SR.

Frequency-dependent Fano factor.—We consider the particle current as the change of the electron number n in a region which may be a lead or the quantum dot, i.e., $j = \dot{n}$. Its symmetrized autocorrelation function $S(t, t') = \frac{1}{2} \langle [\Delta j(t), \Delta j(t')]_+ \rangle$ in the stationary limit, must obey the discrete time-translation invariance of the Liouvillian, namely, $S(t, t') = S(t+T, t'+T)$. By introducing the time difference $\tau = t - t'$, one sees that $S(t, t - \tau)$ is invariant under $t \rightarrow t+T$, i.e., for constant τ it is T periodic in t [21]. This implies that time averages over a driving period are equivalent to averages over the phase of the driving [22]. Hence, we define the phase-averaged correlation function $\bar{S}(\tau) \equiv \overline{S(t+\tau, t)^t} = \overline{S(t, t-\tau)^t}$, where the second equality follows readily from simultaneous translation of all times. The corresponding phase-averaged spectral density $\bar{S}(\omega)$ is normalized to the average current \bar{I} to yield as dimensionless noise spectrum the frequency-dependent Fano factor $F(\omega) = \bar{S}(\omega)/\bar{I}$, which is our main quantity of interest.

To compute $\bar{S}(\omega)$, we establish its relation to the conditional second moment of the electron number in the lead as $M_2(t|t') = \langle \Delta n^2(t) \rangle_{t'}$, where the subscript t' denotes the reference time from which on we consider the fluctuations. Owing to $\dot{n}(t) = j(t)$, one finds

$$M_2(t|t_0) = \int_{t_0}^t dt'' \int_{t_0}^{t''} dt' S(t'', t'), \quad (2)$$

whose time derivative is the conditional second current cumulant $c_2(t|t_0) = 2 \int_{t_0}^t dt' S(t, t')$. Via the substitution $t' \rightarrow t' - \tau$, a subsequent phase average, and Fourier transformation, we obtain the generalized MacDonald formula [23]

$$\bar{S}(\omega) = \omega \int_0^\infty d\tau \sin(\omega\tau) \int_0^T \frac{dt}{T} c_2(t+\tau|t). \quad (3)$$

The remaining task is the computation of the time evolution of the conditional current cumulant c_2 for sufficiently many values of t (or initial phases).

For this purpose, we employ a propagation method for the full-counting statistics [29]. It is based on a master equation for a reduced density operator $X(\chi, t)$ augmented by a counting variable χ such that $X(0, t) \equiv \rho(t)$. By construction, its trace is the cumulant generating function [30] of the transported electrons. In particular, the first two Taylor coefficients of $(d/dt)X(\chi, t)$ provide the current and the second current cumulant. While the longtime dynamics of $X(\chi, t)$ yields the zero-frequency noise considered in

Ref. [29], here we are interested in stationary correlations which depend on transients. Therefore, the initial condition of X deserves some attention. First, stationarity requires that at initial time t' , transients of the density operator $\rho(t)$ must have decayed. Second, the conditional cumulants are initially zero. The choice $X(\chi, t') = \rho_{\text{stat}}(t')$ fulfills both conditions. For a detailed derivation, see the Supplemental Material [23].

Power spectrum of the measured current.—With the experimentally determined times at which the electrons tunnel, we perceive the total current I as well as I_L and I_R as spike trains. In the absence of the driving, the power spectrum of such spike train can be computed from the distribution function of the waiting times between subsequent events [11,12,31,32]. We generalize this relation to the periodically time-dependent case to obtain the phase-averaged power spectrum of an ac-driven spike train [23],

$$\bar{S}(\tau) = \bar{\gamma}\delta(\tau) + \bar{\gamma}w(|\tau|) + \varphi(|\tau|), \quad (4)$$

where the first term is the δ -correlated shot noise for the mean spike rate $\bar{\gamma}$. $w(\tau) = \sum_{\ell} w_{\ell}(\tau)$ is given by the probability distributions of the waiting times between a tunnel event and its $(\ell + 1)$ st successor $w_{\ell}(\tau)$, which we sample from experimental data. Notably, the $w_{\ell}(\tau)$ oscillate with the driving frequency [33].

For φ we only know that it is T periodic and has zero mean [23]. Without the driving, it vanishes such that Eq. (4) recovers a result from renewal theory [11,12]. To determine φ , we notice that for large time difference τ , the tunnel events are uncorrelated and, thus, \bar{S} vanishes. Therefore, φ can be identified with the longtime oscillations of $w(\tau)$. Accordingly, in the frequency domain we use the fact that finite-time Fourier transformation converts longtime oscillations to poles of first order, while $\bar{S}(\omega)$ is expected to be a smooth function. Therefore, poles in the Fourier transformed of $w(\tau)$ can be attributed to φ . They can be determined by fitting.

SR signatures in the Fano factor.—In Ref. [7], the existence of SR in quantum transport has been demonstrated with the zero-frequency Fano factor as a noise measure. However, a complete picture must include its full spectral properties. As a reference, let us mention that in the absence of driving, the current in a symmetric quantum dot has white noise characterized by the constant Fano factor $F(\omega) = 1/2$ [34–36]. Moreover, for adiabatic driving, most of the time the symmetry gets lost such that the zero-frequency noise is enhanced [37]. Since we are interested in SR, we consider much larger frequencies of the order Γ_0 . Figure 2(a) shows noise spectra of the total current for various nonadiabatic driving frequencies. For the relatively small $f = 0.4$ kHz, the zero-frequency noise is already below the standard value $1/2$ expected for the undriven dot. Slightly away from $\omega = 0$, however, $F(\omega) > 1/2$. With increasing f , the dip in the noise

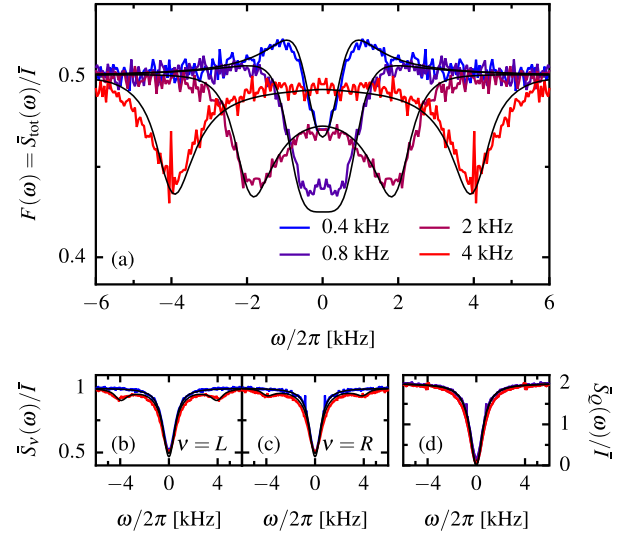


FIG. 2. Frequency-dependent Fano factor, i.e., normalized power spectrum of the total current (a), the current at source (b), drain (c), and the net current to the dot (d) for driving amplitude $A = 10$ meV and various driving frequencies. The colored lines mark experimental data, while the black lines are computed with the master equation approach. The other parameters are $\alpha_L = 0.09$, $\alpha_R = 0.065$, and $\Gamma_0 = 1.675$ kHz.

spectrum at $\omega = 0$ becomes deeper and broader. Close to the SR condition $f \approx \Gamma_0/2$, it evolves into a double dip located at $\omega = \pm 2\pi f$, which underlines the importance of considering the whole noise spectrum. While the zero-frequency noise insinuates disappearance of the SR effect, the frequency-dependent analysis reveals that the noise suppression remains, but occurs in the spectrum at finite frequency. In contrast, the current noise at source and drain depends only weakly on the driving, as can be seen in Figs. 2(b) and 2(c). Only when the driving frequency exceeds the SR frequency, i.e., for $f \gtrsim \Gamma_0/2$, the Fano factor of $I_{L/R}$ develops small dips at $\omega \approx \pm 2\pi f$. Interestingly, the noise of the dot current [Fig. 2(d)] and, thus, that of the dot occupation are practically independent of the driving. This emphasizes that for transport SR, the noise properties are primarily manifest in the total current.

The magnitude and the position of the noise reduction are analyzed in Fig. 3. Panels 3(a) and 3(b) show how the minimum of $F(\omega)$, as observed in Fig. 2(a), changes with the driving frequency f . The data confirm that the minimum of the Fano factor in the adiabatic limit, i.e., for low driving frequency, assumes values considerably larger than the standard value $1/2$, as discussed above. Upon increasing the driving frequency, the minimum becomes lower until at an amplitude-dependent value f_{min} , it starts to increase again. Figure 3(b) shows good agreement between theory and experiment for the development of the minimum of the Fano factor for an amplitude $A = 10$ meV considering a certain noise in the experimental data. In particular, the data clearly confirm the frequency independence of the

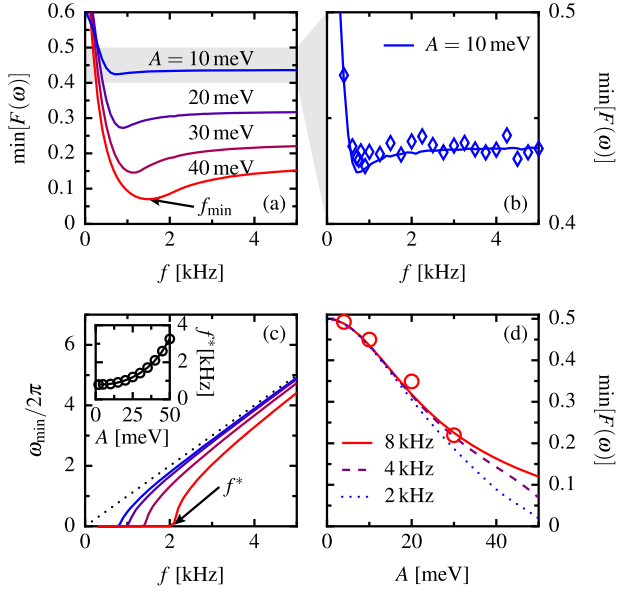


FIG. 3. Analysis of the dips in the noise spectra. (a) Minimum of the Fano factor $F(\omega)$ for various amplitudes as function of the driving frequency. (b) Enlargement of the shaded area in panel (a) together with corresponding experimental data indicated by diamonds. (c) Frequency at which the minimum is located in the power spectrum for the data in panel (a). Inset: transition frequency f^* as function of the driving amplitude. (d) Minimum of the Fano factor as function of the driving amplitude for various driving frequencies. The circles mark experimental results for $f = 8$ kHz. All other parameters are as in Fig. 2.

minimum beyond the SR point. Next, we consider the location of the minimum in the spectrum ω_{\min} depicted in Fig. 3(c), where the transition from $\omega_{\min} = 0$ to a finite value corresponds to the splitting of the dip as observed in Fig. 2(a). This happens at a frequency f^* which increases with increasing driving amplitude. The inset of Fig. 3(c) depicts the dependence on the driving amplitude. The growth of f^* with the driving amplitude reminds one of the shift of the optimal working point known from the “usual” SR in closed systems [2].

Figure 3(d) depicts the minimum of the Fano factor as a function of the driving amplitude for three driving frequencies (beyond the SR condition). A strong reduction of the Fano factor is clearly observed in accordance with experimental data for 8 kHz [38]. At strong driving, the reduction is enhanced for frequencies closer to the SR condition, compare the curves for 2 and 8 kHz.

To investigate the amplitude dependence in more detail, we present in Fig. 4(a) the frequency dependent Fano factor at three different applied amplitudes and a driving frequency much larger than f^* . The curves exhibit the double-dip structure discussed above. With an increasing amplitude, the shape of the Fano factor starts to deviate from the Lorentzian obtained for weak driving. Moreover, for $A = 30$ meV, we witness an impact of nonlinearities visible as tiny additional dip at $\omega/2\pi \approx 3f$. In the

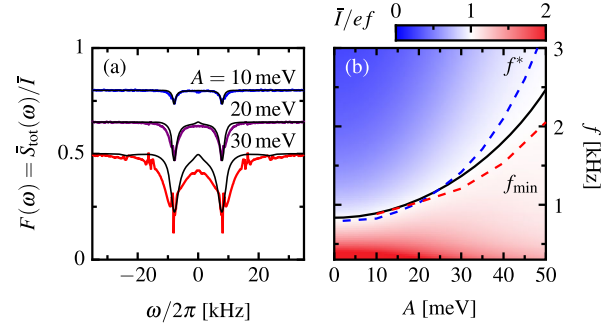


FIG. 4. (a) Frequency-dependent Fano factor of the total current for $f = 8$ kHz and various amplitudes. All other parameters are as in Fig. 2. The curves for 10 and 20 meV are vertically shifted by 0.15 and 0.3, respectively. (b) Transported charge per driving period, where the solid line highlights parameters with quantized current $\bar{I} = ef$. The dashed lines mark the transition frequency f^* as a function of the amplitude [see inset of Fig. 3(c)] and the frequency f_{\min} at which for given A the Fano factor assumes its minimum [cf. Fig. 3(a)].

experimental data the additional dip is less clear, because the large driving amplitude makes it increasingly difficult to determine with sufficient precision the poles stemming from the last term in Eq. (4). The increased broadening of the dips with increasing amplitude is, by contrast, even more expressed in the experimental data.

Recent interest in controlled single-electron tunneling stems from the challenge of building current standards [15] that transport a definite number of electrons per cycle. Let us therefore discuss our observations in this context. Figure 4(b) shows the average (electric) current as a function of the driving amplitude and frequency. In the same figure also the desired quantized current $\bar{I} = ef$ (black line) and the above discussed frequencies f_{\min} and f^* are shown as a function of the driving amplitude. For amplitudes $A \lesssim 20$ meV, the three lines more or less overlap, i.e., there is no clear difference between f_{\min} and f^* and they mark the quantized current. For larger amplitudes a plateaulike structure with $\bar{I} \approx ef$ is observed [white region in Fig. 4(b)] as expected from the experiments investigating single-electron pumping for current standards [15]. The line on which $\bar{I} = ef$ is fulfilled exactly lies in the middle of this plateau and between f^* and f_{\min} . With increasing amplitude, both the width of the plateau and the difference between f_{\min} and f^* become larger. Accordingly, for large frequencies, very low Fano factors require larger amplitudes, see Fig. 3(d). Such a plateau widening with increasing amplitude was also observed in the pumping experiments investigating current standards [13,14]. Interestingly, the two frequencies f_{\min} and f^* mark the borders of the plateau. In this way an analysis of the frequency dependent Fano factor can help to optimize the pumping conditions for current standards.

Conclusions.—We have analyzed experimentally and theoretically the frequency dependent current noise in a

transport SR experiment. The most noticeable effect is visible in the power spectrum of the total current as a splitting of a dip at zero frequency to a double dip located at the driving frequency. For small amplitudes, the transition between these two qualitatively different regimes occurs when the SR condition is met. With increasing amplitudes, the transition frequency shifts toward larger values. Our results show the relation between transport SR and quantized electron pumping used for current standards.

This work was supported by the Zukunftscolleg of the University of Konstanz and by the Spanish Ministry of Science, Innovation, and Universities under Grant No. MAT2017-86717-P and the CSIC Research Platform on Quantum Technologies PTI-001, by the Deutsche Forschungsgemeinschaft (DFG, German Research Foundation) under Germany's Excellence Strategy—EXC-2123 Quantum Frontiers—390837967, and by the State of Lower Saxony, Germany, via Hannover School for Nanotechnology and School for Contacts in Nanosystems.

-
- [1] P. Jung and P. Hänggi, *Phys. Rev. A* **44**, 8032 (1991).
 [2] L. Gammaitoni, P. Hänggi, P. Jung, and F. Marchesoni, *Rev. Mod. Phys.* **70**, 223 (1998).
 [3] F. Moss, L. M. Ward, and W. G. Sannita, *Clin. Neurophysiol.* **115**, 267 (2004).
 [4] M. Grifoni and P. Hänggi, *Phys. Rev. Lett.* **76**, 1611 (1996).
 [5] T. Wellens and A. Buchleitner, *Phys. Rev. Lett.* **84**, 5118 (2000).
 [6] C. K. Lee, L. C. Kwek, and J. Cao, *Phys. Rev. A* **84**, 062113 (2011).
 [7] T. Wagner, P. Talkner, J. C. Bayer, E. P. Rugeramigabo, P. Hänggi, and R. J. Haug, *Nat. Phys.* **15**, 330 (2019).
 [8] C. Emary, D. Marcos, R. Aguado, and T. Brandes, *Phys. Rev. B* **76**, 161404(R) (2007).
 [9] D. Marcos, C. Emary, T. Brandes, and R. Aguado, *New J. Phys.* **12**, 123009 (2010).
 [10] R. Hussein, J. Gómez-García, and S. Kohler, *Phys. Rev. B* **90**, 155424 (2014).
 [11] D. R. Cox, *Renewal Theory* (Methuen & Co., London, 1962).
 [12] W. Gerstner, W. M. Kistler, R. Naud, and L. Paninski, *Neuronal Dynamics* (Cambridge University Press, Cambridge, England, 2014).
 [13] M. D. Blumenthal, B. Kaestner, L. Li, S. Giblin, T. J. B. M. Janssen, M. Pepper, D. Anderson, G. Jones, and D. A. Ritchie, *Nat. Phys.* **3**, 343 (2007).
 [14] B. Kaestner, V. Kashcheyevs, G. Hein, K. Pierz, U. Siegner, and H. W. Schumacher, *Appl. Phys. Lett.* **92**, 192106 (2008).
 [15] B. Kaestner and V. Kashcheyevs, *Rep. Prog. Phys.* **78**, 103901 (2015).
 [16] S. Platonov, B. Kästner, H. W. Schumacher, S. Kohler, and S. Ludwig, *Phys. Rev. Lett.* **115**, 106801 (2015).
 [17] S. Ramo, *Proc. IRE* **27**, 584 (1939).
 [18] W. Shockley, *J. Appl. Phys.* **9**, 635 (1938).
 [19] Y. M. Blanter and M. Büttiker, *Phys. Rep.* **336**, 1 (2000).
 [20] C. Bruder and H. Schoeller, *Phys. Rev. Lett.* **72**, 1076 (1994).
 [21] S. Kohler, J. Lehmann, and P. Hänggi, *Phys. Rep.* **406**, 379 (2005).
 [22] P. Jung and P. Hänggi, *Phys. Rev. A* **41**, 2977 (1990).
 [23] See Supplemental Material at <http://link.aps.org/supplemental/10.1103/PhysRevLett.125.206801>, which includes Refs. [24–28], for a derivation of the formalism and the relation between $\tilde{S}(\omega)$ and the waiting time distributions.
 [24] D. K. C. MacDonald, *Rep. Prog. Phys.* **12**, 56 (1949).
 [25] H. Risken, *The Fokker-Planck Equation*, Springer Series in Synergetics, 2nd ed., Vol. 18 (Springer, Berlin, 1989).
 [26] C. Flindt, T. Novotný, A. Braggio, M. Sassetti, and A.-P. Jauho, *Phys. Rev. Lett.* **100**, 150601 (2008).
 [27] C. Flindt, T. Novotný, A. Braggio, and A.-P. Jauho, *Phys. Rev. B* **82**, 155407 (2010).
 [28] A. A. Clerk and S. M. Girvin, *Phys. Rev. B* **70**, 121303(R) (2004).
 [29] M. Benito, M. Niklas, and S. Kohler, *Phys. Rev. B* **94**, 195433 (2016).
 [30] D. A. Bagrets and Y. V. Nazarov, *Phys. Rev. B* **67**, 085316 (2003).
 [31] N. G. van Kampen, *Stochastic Processes in Physics and Chemistry* (North-Holland, Amsterdam, 1992).
 [32] T. Brandes, *Ann. Phys. (Amsterdam)* **17**, 477 (2008).
 [33] F. Brange, A. Schmidt, J. C. Bayer, T. Wagner, C. Flindt, and R. J. Haug, [arXiv:2005.06176](https://arxiv.org/abs/2005.06176).
 [34] A. N. Korotkov, *Phys. Rev. B* **49**, 10381 (1994).
 [35] S. Gustavsson, R. Leturcq, B. Simović, R. Schleser, T. Ihn, P. Studerus, K. Ensslin, D. C. Driscoll, and A. C. Gossard, *Phys. Rev. Lett.* **96**, 076605 (2006).
 [36] N. Ubbelohde, C. Fricke, C. Flindt, F. Hohls, and R. J. Haug, *Nat. Commun.* **3**, 612 (2012).
 [37] R.-P. Riwar, J. Splettstoesser, and J. König, *Phys. Rev. B* **87**, 195407 (2013).
 [38] As the experimental spectra are noisy, we have convoluted them with a Gaussian of width $\sigma = 100$ Hz before reading off the minima.